Thin Solid Films, *91* (1982) 163–173
METALLURGICAL AND PROTECTIVE COATINGS

REACTIVE SPUTTER-COATED REACTION-BONDED SILICON NITRIDE

O. J. GREGORY AND M. H. RICHMAN
Division of Engineering, Brown University, Providence, RI 02912 (U.S.A.)
(Received December 23, 1981; accepted January 20, 1982)

A coating technique was developed to provide high temperature oxidation resistance and hot corrosion resistance to gas turbine components made of reaction-bonded silicon nitride. Thick coatings of reactively sputtered silicon nitride were deposited onto reaction-bonded silicon nitride surfaces to form an effective oxygen diffusion barrier by eliminating all potential short-circuit paths. To accomplish this, hard crystalline coatings were produced by subsequent heat treatment of the as-deposited silicon nitride. The as-deposited and annealed films were characterized by a variety of methods to determine the phase content, extent of crystallinity, grain size and morphology. With this coating technique, the oxidation of the underlying silicon nitride was substantially reduced in the temperature range 1000–1200 °C.

1. INTRODUCTION

For the past decade, reaction-bonded silicon nitride (RBSN) has been investigated as a replacement material for superalloys in gas turbine engines. The use of such ceramic components under the proposed operating temperatures (1000–1370 °C) can lead to considerable oxidation and premature failure. RBSN contains both surface and subsurface porosity. Surface pores can act as sites for oxidation and can cause the initiation of tensile cracks at the surface. These pores therefore represent Griffith flaws which can propagate under the influence of hydrostatic tensile stresses that develop during thermal oxidation. Subsurface oxidation can also lead to similar consequences. If this subsurface porosity is connective, oxidation is governed by kinetics similar to those of surface oxidation. If it is non-connective, considerable solid state diffusion must take place to cause oxide formation in these isolated pores. Cristobalite, the stable oxide usually formed by oxidation at these temperatures, undergoes a displacive transformation at 270 °C when the high temperature phase (β) transforms to the low temperature phase (α) and this transformation is accompanied by a 5% increase in specific volume. While the oxidation of RBSN has been investigated by several researchers[1,2], little attention has been paid to the development of coatings or treatments to protect against oxidation and corrosion.

The protection system presented in this paper consists of the deposition onto a

0040-6090/82/0000-0000/$02.75

porous RBSN surface of a hard dense film of crystalline Si_3N_4 by reactive sputtering. This film effectively seals off the surface and prevents oxidation of the underlying material by forming a barrier to oxygen diffusion. Several alternative methods such as chemical vapor deposition (CVD), prior oxidation at elevated temperatures and impregnation have been suggested[3–5].

However, there are advantages and disadvantages to each method. The chief advantages to the reactive sputtered protective coating system described are (1) the capability of depositing thick bulk films without spalling (reactive sputtering produces residual compressive stresses within the film, while CVD produces residual tensile stresses), (2) the ability to atomically clean the substrate by etch bias sputtering prior to deposition (for better adhesion) and (3) close control over stoichiometry and impurities in the coatings. The chief disadvantages are (1) the slow deposition rates and (2) the long preparation times required for any high vacuum work. The main advantages of CVD are (1) the relatively fast deposition rates, (2) the absence of geometry or size limitations and (3) the lack of the requirement for a vacuum. The major disadvantages of CVD are (1) the corrosive nature of the reactant gas mixtures, (2) possible attack of the substrate and (3) the use of toxic and expensive reactant gases. Prior oxidation to form a protective barrier at temperatures below the application temperature can be easily accomplished, but the oxide formed at high temperatures will eventually undergo the $\alpha \rightarrow \beta$ transformation upon thermal cycling. Silicon impregnation is limited because any excess silicon capable of undergoing oxidation will present similar problems. The advantages in using Si_3N_4, in particular, as the protective material are (1) there is no discrepancy in the coefficients of thermal expansion of the coating and substrate, (2) Si_3N_4 is very stable chemically and (3) Si_3N_4 has a very high hot hardness which reduces erosion–corrosion. In this paper, the reactive sputtering parameters and the characterization of various as-deposited and annealed films are presented. Other aspects of this work, *i.e.* the actual oxidation behavior of the coated RBSN, will be reported in a future paper.

2. EXPERIMENTAL DETAILS

The objective of this work was to produce well-characterized crystalline Si_3N_4 films by the reactive sputtering of high purity polycrystalline silicon in N_2–Ar atmospheres. Since the diffusion of oxygen through a crystalline oxide is more difficult than through a similar amorphous oxide[6], and since crystalline coatings are harder and more wear resistant than the corresponding amorphous ones, a totally crystalline coating was desired. Consequently, a post-sputtering heat treatment was necessary. (Crystalline Si_3N_4 films can be achieved when the substrate temperature exceeds 900 °C. A maximum substrate temperature of 600 °C was achievable in this apparatus and therefore was not high enough to produce a crystalline coating.) The coatings were characterized both before and after heat treatment by IR analysis, X-ray diffraction (XRD) analysis and scanning and transmission electron microscopy (SEM and TEM). The coated RBSN samples were then oxidized under ambient conditions at 1000 and 1200 °C.

The substrates were prepared by metallographic polishing followed by ultrasonic cleaning in acetone and methanol. An MRC 822 Sputtersphere r.f. sputtering unit was used with an operating frequency of 13.56 MHz. (A polycrystalline silicon target (99.99% Si) supplied by MRC was used for all runs. The target was fabricated by cold pressing silicon powder to minimize contamination.) The operating chamber was evacuated to less than 2.2×10^{-7} Torr and backfilled with mixtures of spectroscopy grade N_2 (less than 0.0004% O_2) and ultrahigh purity argon. Si_3N_4 coating rates as large as 550 Å min^{-1} could be realized by varying the power density, substrate temperature, bias potential, argon-to-nitrogen ratio and total gas pressure. The final thicknesses of the coatings were varied from 1 to 10 μm to determine an optimal barrier thickness.

The as-deposited amorphous or partially crystalline Si_3N_4 films were annealed in Ar–N_2 mixtures which had been dried over P_2O_5 and gettered for O_2. (A Thermox oxygen meter capable of determining oxygen levels as low as 0.1 ppm was used to measure the oxygen content in the furnace system. Typical oxygen contents were 0.0004% or less.) Heating these films above 1000 °C can result in the decomposition of the nitride and therefore N_2 gas was added to reverse this reaction. A programmable heating–cooling rate of 50 °C h^{-1} was used to prevent viscous flow of the glassy layer due to the outgassing of argon trapped during the sputtering process. The deposition rate was determined by coating a glass slide for 1 h and measuring the thickness. A "stylus" Dektak step profiler and a Talysurf 4 surface profilometer were used to measure the thickness by running the stylus over a virgin glass surface and then over an edge of the coating. Ellipsometry was used to check the thickness obtained by this method and to determine the index of refraction. All measurements were made using an automatic ellipsometer (Rudolph Research Auto EL II).

The morphologies of the as-coated and annealed films were examined using both SEM and TEM. A JEM-7 transmission electron microscope was used to determine the extent of crystallinity, the grain size and crystal growth during annealing. The effect of electron-beam-induced crystallization was minimized by exposing the areas of interest for only short periods of time. Selected area diffraction was performed to determine the crystallinity of various regions. Thin films were obtained by scraping non-coherent films from the as-deposited slides and annealing them between two Si_3N_4 plates to prevent buckling. These films were cut to fit a 75 mesh TEM grid, were wet with epoxy and were placed on the grid to cure. The samples were then reduced in thickness in an ion beam mill at an incident angle of 15°. They were ion milled to the point where holes appeared in the film (current, 5 mA; voltage, 3 kV). After milling, the samples were examined by TEM using an accelerating voltage of 100 kV.

IR analysis was used to determine the various absorption edges corresponding to crystalline and/or amorphous Si_3N_4. All IR analyses were determined on a Perkin–Elmer model 510 IR double-beam ratio recording spectrophotometer. A silicon single-crystal wafer of the same thickness as the substrate was used as a reference to eliminate the substrate absorption bands, thereby allowing direct determination of the absorption edges in the spectra. In addition, a nitrided single-crystal wafer of silicon was used to generate a standard spectrum for comparison.

3. RESULTS AND DISCUSSION

The reactively sputtered coatings of Si_3N_4 in the as-sputtered condition ranged from completely amorphous to partially crystalline depending on the substrate temperature. XRD patterns of the films deposited at low temperatures revealed a single broad peak characteristic of an amorphous material having a crystal size less than 20 Å. XRD patterns of the films deposited at higher temperatures revealed a sharper peak corresponding to a quartet of Si_3N_4 peaks (α102, α210, β101, β210) at 2θ angles between 33° and 37°. A single sharp peak propagating from this broadened peak was frequently observed at high temperatures. This is attributed to an oriented growth direction (perpendicular to the 102 planes) when α-Si_3N_4 is deposited onto the (111) surfaces of single-crystal silicon. Similar preferred orientations have been observed when similar single-crystal silicon has been directly nitrided[7] or coated by CVD techniques[3]. The peak broadening observed in the XRD patterns of the annealed films indicated a range of crystal sizes of the order of 100–400 Å. (In addition, the XRD patterns of the coating showed a peak shift (along the 2θ scale) as large as 0.5°. It has been documented that sputtered films develop residual compressive stresses which enable thick bulk films to be prepared without spalling. Compressive stresses as large as 86 500 lbf in^{-2} were estimated for these films.) These annealed films were analyzed for phase content (the ratio of α phase to β phase and of α phase to silicon) as well.

A coating free of any residual silicon (*i.e.* non-reacted silicon) would provide the greatest protection in terms of oxidation resistance and hot corrosion resistance. The presence of residual silicon in Si_3N_4 sputtered films is well documented[8,9] and therefore an effort was made to minimize the percentage of residual silicon. Two different techniques were used to determine the residual silicon. First, the index of refraction of the as-deposited films, determined by ellipsometry (6300 Å) and a fringing technique, was correlated with the amount of residual silicon ($\eta_{Si} = 3.85$; $\eta_{Si_3N_4} = 2.1$). Alternatively, the films were annealed at high temperatures for long times (1300–1370 °C for 200 h) and analyzed by XRD using a quantitative phase analysis[10] to determine the relative amounts of α-Si_3N_4, β-Si_3N_4 and silicon from X-ray peak intensities. The effects of nitrogen partial pressure and deposition temperature on the residual silicon content are shown in Figs. 1 and 2.

The Si_3N_4 deposition rates were much greater than those employed by other researchers[11], who used essentially pure nitrogen as the sputtering gas. In about 90 min, a film 4 μm thick exhibiting good adhesion could be deposited. This sputtering efficiency was directly related to the target size, geometry and power density used. Figure 3 shows the influence of the power density and of the partial pressure of the argon gas (ionizing gas) on the deposition rate for this system. Increased rates can be achieved by increasing the argon pressure above this limited range. However, too high a partial pressure can lead to argon entrapment in the film and the eventual release of this gas when the film is annealed. Direct observation of the film by SEM after annealing revealed a blistered topography suggesting this release of argon gas.

The bonding between substrate and coating in the as-deposited condition is excellent when the substrate is first sputter etched. Films not prepared in this fashion could be easily removed or scratched. This difference in adhesion is shown in Figs. 4

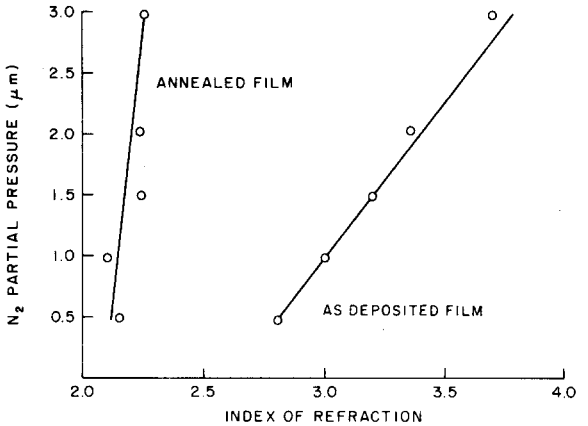

Fig. 1. Effect of the N_2 partial pressure on the Si_3N_4 content in the coating for as-deposited films and annealed (for 100 h at 1000 °C) films ($\eta_{Si_3N_4} = 2.1$; $\eta_{Si} = 3.85$; $T_{dep} = 250$ °C; total pressure, 10 μmHg).

Fig. 2. Effect of the deposition temperature on the Si_3N_4 content in the coating for a 10 μmHg pressure of the gas mixture ($\eta_{Si_3N_4} = 2.1$; $\eta_{Si} = 3.85$): △, 96%N_2–4%H_2; ○, 100%N_2–0%H_2.

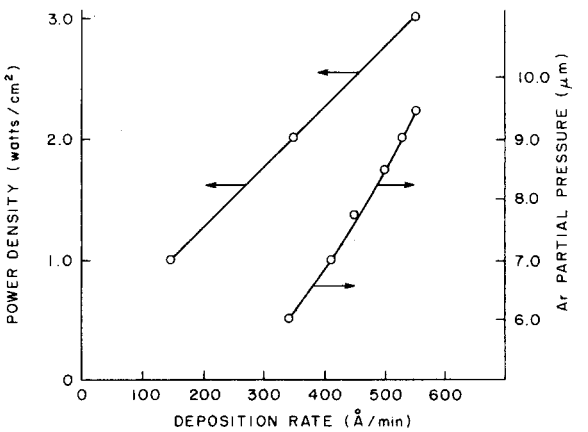

Fig. 3. Effect of the power density and the argon partial pressure on the deposition rate (total pressure, 10 μmHg).

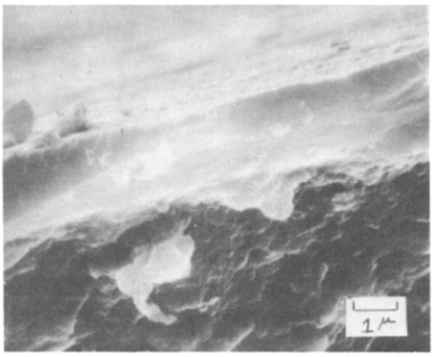

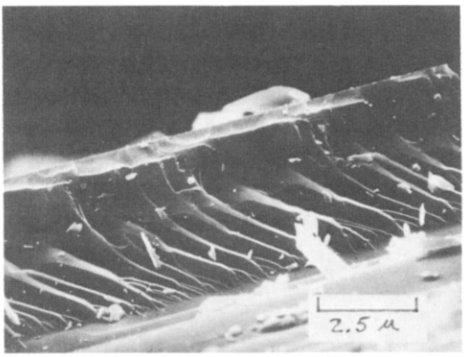

Fig. 4. SEM micrograph of the fracture surface of an as-deposited amorphous Si_3N_4 coating on RBSN. This coherent coating was prepared by etch bias sputtering.

Fig. 5. SEM micrograph of the fracture surface of an as-deposited amorphous Si_3N_4 coating. The river patterns originating at the silicon interface should be noted.

and 5 where etching reveals a coherent film and a lack of etching reveals a non-coherent film. The SEM micrograph of Si_3N_4-coated RBSN (Fig. 4) shows cleavage propagating continuously through the coating. However, a lack of etching results in a step in the fracture surface at the silicon interface (Fig. 5). The formation of river patterns at this interface is a strong indication of poor adhesion. In addition, etching preferentially removes silicon from the substrate. This is due to the fact that the bond strength of the Si—Si bond is less than that of the Si—N bond in Si_3N_4. The implication here is that a lower silicon content in the surface layer of RBSN will retard further oxidation. Reduced amounts of residual silicon in the deposited films can also be achieved by sputtering with a negative bias. Once again, the silicon, having the lower bond strength, will be preferentially re-sputtered.

An SEM investigation of the as-deposited and the annealed surface revealed several interesting morphologies. Rounded protuberances (approximately 1 μm in diameter) were observed on the free surfaces of the Si_3N_4 as shown in Fig. 6. This

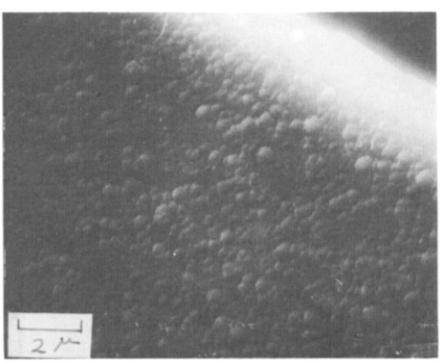

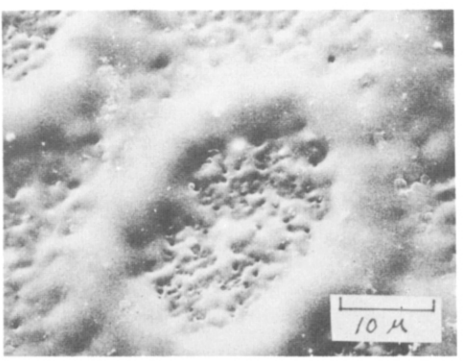

Fig. 6. SEM micrograph of an as-deposited reactively sputtered surface. The rounded protuberances on the surface should be noted.

Fig. 7. SEM micrograph of a blister on the surface of an annealed Si_3N_4 film which developed during the outgassing of trapped argon.

morphology has been observed on numerous r.f.-sputtered films as well as on amorphous CVD films[3]. When the as-deposited films were annealed, several imperfections developed on the surfaces. High temperature annealing (1370 °C) resulted in a glassy surface containing fine pores. One of these blisters which developed during the outgassing of the argon trapped in the film during sputtering is shown in Fig. 7. At these temperatures, the pressure of the gas was sufficient to cause viscous flow of the amorphous Si_3N_4 and ultimate rupture of that film. A negative bias potential (50 V) was introduced to minimize the entrapment of the reactive gas during sputtering and a lower total gas pressure (10 μmHg or less) was maintained in the system to offer less chance for gas entrapment.

The morphology of a crystalline sputtered film is quite different from that of bulk RBSN material. An SEM fractograph of a crystalline coating (Fig. 8(a)) reveals a dense intergranular fracture surface with a glassy surface layer. From this it is apparent that crystallization started from the silicon interface and developed in an outward manner with the free surface remaining glassy. A rough estimate of the resulting grain size (much less than 1 μm) and density of the film can be deduced from the intergranular fracture surface in Fig. 8(b).

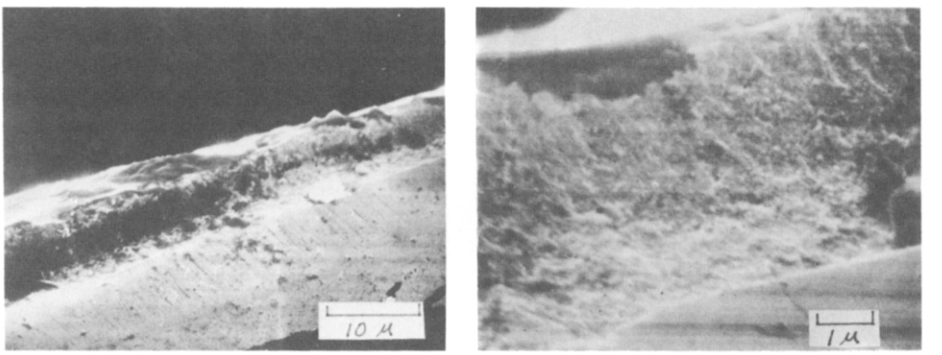

(a) (b)

Fig. 8. SEM micrographs of the fracture surface of an annealed Si_3N_4 coating: (a) granular bulk coating with a glassy surface layer; (b) fine-grained Si_3N_4 showing little porosity.

The average grain size in the annealed films was determined by the deposition conditions and the annealing times and temperatures. In a separate study, though, it was found that a limiting grain size quickly develops after which there is little further grain growth. A typical thin film having an average grain size of 400 Å is shown in Fig. 9. Also, duplex grain structures were frequently observed in the annealed films.

The rounded protuberances or surface intersections of the as-deposited amorphous films with well-defined boundaries are shown in the TEM micrograph of Fig. 10. There is evidence that the final grain size of the Si_3N_4 grains is controlled by the size of the amorphous "island" and that the Si_3N_4 crystallites are nucleated within these regions. The final grain size established in these coatings was not limited by the thickness of the film, as the thickness was several orders of magnitude greater than the average grain size determined by metallography (500 Å compared with 10 000–100 000 Å). A partially crystallized film (Fig. 11(a)) shows extensive nucleation within these regions and the absence of crystallites adjacent to the

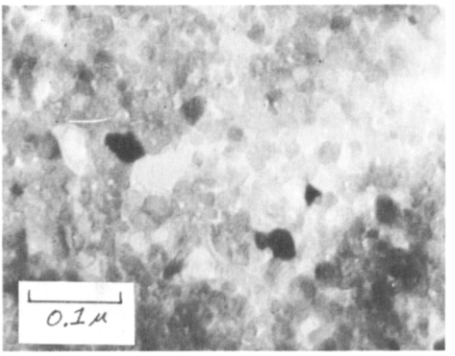

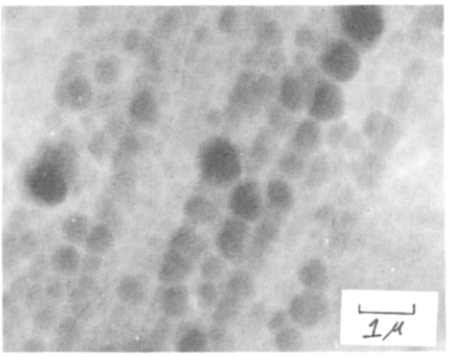

Fig. 9. TEM micrograph of an annealed Si_3N_4 coating exhibiting a fine-grained structure.

Fig. 10. TEM micrograph of an as-deposited amorphous coating showing the size of the rounded protuberances.

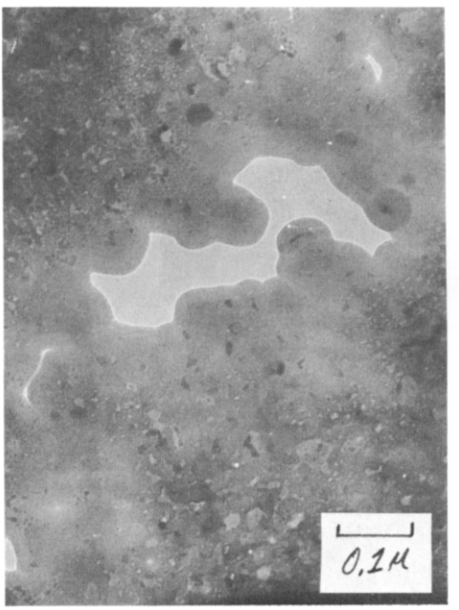

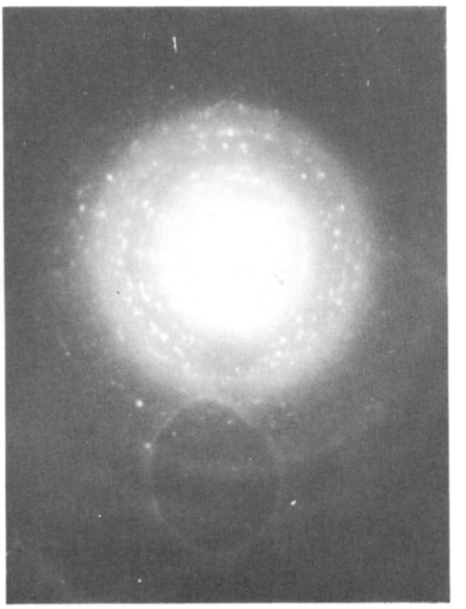

(a) (b)

Fig. 11. (a) TEM micrograph and (b) electron diffraction pattern of a partially crystallized coating, showing an amorphous nature at a triple junction and extensive crystallization at interior regions.

amorphous boundaries. The accompanying electron diffraction pattern (Fig. 11(b)) provides corroboration. The extent of crystallinity during annealing was determined by quantitative metallography. An annealed film determined to be 30% crystalline (100 h at 1300 °C) is shown in Fig. 12.

IR spectroscopy was used to determine the extent of crystallinity during the annealing process. The as-deposited films, being amorphous in nature, do not absorb IR radiation at characteristic wavelengths. Consequently, the IR spectra of these films do not exhibit sharp peaks since there is considerable variation in

interatomic distances. As a film becomes more crystalline, stronger Si—N bonds approach the crystalline absorption edges. The development of characteristic peaks and their increase in both intensity and sharpness shows the Si_3N_4 amorphous-to-crystalline transition. IR spectra showing one such transition in an Si_3N_4 film prepared by r.f. sputtering (0.5%N_2–0.5%Ar) are shown in Fig. 13. IR analysis was also used as an indirect check on the silicon content and microporosity in the films;

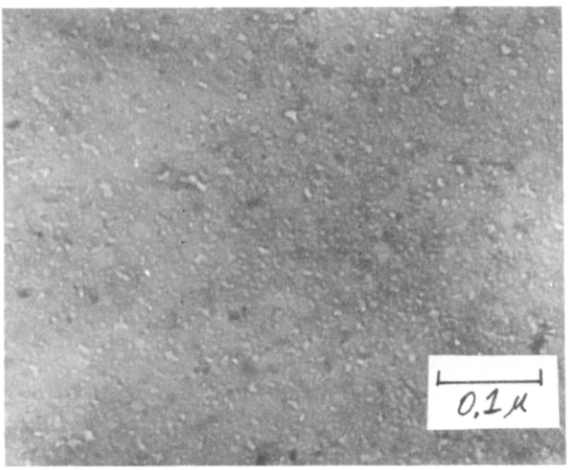

Fig. 12. TEM micrograph of a partially crystallized coating (approximately 30% crystalline).

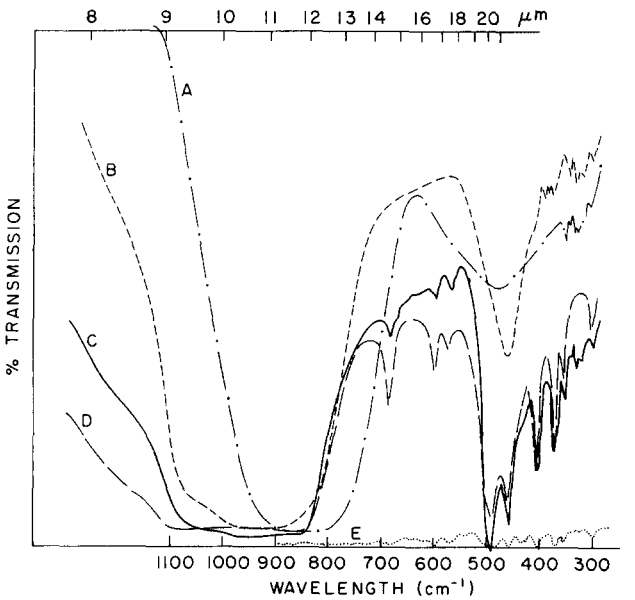

Fig. 13. IR spectra of an Si_3N_4 film (deposited in 5%N_2–95%Ar at T = 250 °C with a power density of 3 W cm^{-2}) showing the amorphous-to-crystalline transition during annealing: curve A, as-deposited film; curve B, film annealed for 96 h (1000 °C); curve C, film annealed for 102 h (1150 °C); curve D, film annealed for 18 h (1300 °C); curve E, film annealed for 200 h (1370 °C).

an absorption edge shift (770–900 cm^{-1}) was an indication of increased silicon content and porosity.

The coatings applied so far have shown the ability to retard oxidation. Coatings of 5 μm or less were sufficient to reduce the amount of oxide converted from the RBSN by 75%. This was accomplished in part by forming an oxygen diffusion barrier to seal off grain boundaries and pores, thereby eliminating all short-circuit paths. This effectively increases the oxygen diffusion path in the RBSN and thus the oxidation rate is reduced. Reducing the amount of residual silicon and depositing thicker coatings should provide still further improvements. This may be accomplished in part by adding H_2 to the reactive gas mixture to increase the rate of reaction above the substrate or by reactively sputtering Si_3N_4 using an RBSN target made by nitriding high purity silicon. Furthermore, small oxygen additions to the reactive gas mixture to produce interstitial oxygen in the Si_3N_4 structure will decrease the diffusivity of oxygen through the coating as well. The preliminary results of these experiments indicate that these methods yield even better oxidation resistance than does the deposition of Si_3N_4 films employed thus far.

4. CONCLUSION

Commercially produced RBSN contains residual silicon and exhibits extensive porosity, both of which enhance its oxidation at high temperatures. Using a reactive sputtering process, well-characterized coatings of Si_3N_4 were applied to RBSN. These Si_3N_4 coatings are deposited amorphously and must be heat treated to become crystallized. The oxidation rate of the sputter-coated RBSN was substantially decreased when a 5 μm thick coating was applied.

ACKNOWLEDGMENT

This work was supported by the Materials Research program at Brown University which is funded by the National Science Foundation.

REFERENCES

1 S. C. Singhal, Oxidation and corrosion–erosion behavior of Si_3N_4 and SiC. In J. J. Burke, A. E. Gorum and R. N. Katz (eds.), *Ceramics for High Temperature Applications*, Brook Hill Publishing, Chestnut Hill, MA, 1974, pp. 533–548.
2 M. G. Mendiratta and H. C. Graham, Strength and fracture toughness of oxidized reaction-bonded Si_3N_4, *Am. Ceram. Soc., Bull., 60* (6) (1981) 623–628.
3 F. S. Galasso, Pyrolytic silicon nitride prepared from reactant gases, *Powder Metall. Int., 11* (1) (1979) 7–9.
4 W. Zdaniewski, D. P. H. Hasselman, H. Knoch and J. Heinrich, Effect of oxidation on the thermal diffusivity of reactor sintered silicon nitride, *Am. Ceram. Soc., Bull., 58* (5) (1979) 539–540.
5 Y. Inomata, Oxidation resistant Si-impregnated surface layer on reaction sintered silicon nitride articles, *Yogyo Kyokai Shi, 83* (1975) 1–3.
6 J. A. Costello and R. E. Tressler, Oxidation kinetics of hot pressed and sintered β-SiC, *J. Am. Ceram. Soc., 64* (6) (1981) 327–331.
7 O. J. Gregory and M. H. Richman, Nitridation of high purity single-crystal silicon, *Metallography, 15* (2) 89–94.
8 J. T. Milek, Silicon nitride for microelectronic applications, in *Handbook of Electronic Materials*, Vol. 3, IFI/Plenum, New York, 1971, p. 38.

9 L. F. Cordes, Evidence of excess silicon in reactively sputtered silicon nitride films, *Appl. Phys. Lett.*, *11* (12) (1967) 383–385.
10 C. P. Gazzera and D. R. Messier, Quantitative determination of phase content of silicon nitride by X-ray diffraction analysis, *AMMRC Tech. Rep. 75-4*, February 1975 (Army Materials and Mechanics Research Center, Watertown, MA).
11 S. M. Hu and L. V. Gregor, Silicon nitride films by reactive sputtering, *J. Electrochem. Soc.*, *114* (8) (1967) 826–833.